

## Structural characterization of human aryl sulphotransferases

Lulu A. BRIX\*, Ronald G. DUGGLEBY†, Andrea GAEDIGK‡ and Michael E. McMANUS\*<sup>1</sup>

\*Department of Physiology and Pharmacology, University of Queensland, Brisbane, Queensland, 4072, Australia, †Department of Biochemistry, University of Queensland, Brisbane, Queensland, 4072, Australia, and ‡The Children's Mercy Hospital, Department of Clinical Pharmacology and Toxicology, Kansas City, MO 64108, U.S.A.

Human aryl sulphotransferase (HAST) 1, HAST3, HAST4 and HAST4v share greater than 90% sequence identity, but vary markedly in their ability to catalyse the sulphonation of dopamine and *p*-nitrophenol. In order to investigate the amino acid(s) involved in determining differing substrate specificities of HASTs, a range of chimaeric HAST proteins were constructed. Analysis of chimaeric substrate specificities showed that enzyme affinities are mainly determined within the N-terminal end of each HAST protein, which includes two regions of high sequence divergence, termed Regions A (amino acids 44–107) and B (amino acids 132–164). To investigate the substrate-binding sites of HASTs further, site-directed mutagenesis was performed on HAST1 to change 13 individual residues within these two regions to the HAST3 equivalent. A single amino acid change in HAST1 (A146E) was able to change the specificity for *p*-nitrophenol to that of HAST3. The substrate specificity of HAST1 towards dopamine could not be converted into that of HAST3 with a single amino acid change. However, compared with wild-type

HAST1, a number of the mutations resulted in interference with substrate binding, as shown by elevated  $K_i$  values towards the co-substrate 3'-phosphoadenosine 5'-phosphosulphate, and in some cases loss of activity towards dopamine. These findings suggest that a co-ordinated change of multiple amino acids in HAST proteins is needed to alter the substrate specificities of these enzymes towards dopamine, whereas a single amino acid at position 146 determines *p*-nitrophenol affinity. A HAST1 mutant was constructed to express a protein with four amino acids deleted (P87–P90). These amino acids were hypothesized to correspond to a loop region in close proximity to the substrate-binding pocket. Interestingly, the protein showed substrate specificities more similar to wild-type HAST3 than HAST1 and indicates an important role of these amino acids in substrate binding.

Key words: chimaeric protein, dopamine, enzyme kinetics, mutagenesis, *p*-nitrophenol.

### INTRODUCTION

Sulphonation is an important reaction in the biotransformation of numerous endo- and xenobiotics, such as neurotransmitters, steroid hormones, drugs and chemical carcinogens [1–3]. The sulphonation reaction involves transfer of a sulphuryl group from the donor substrate 3'-phosphoadenosine 5'-phosphosulphate (PAPS) to the acceptor substrate and is catalysed by a superfamily of enzymes called sulphotransferases (STs) [1–3]. To date, 30 different cytosolic STs have been cloned from various species [4] and sequence alignment of these has revealed at least two regions of highly conserved amino acids; PKSGTXW near the N-terminal end, and RKGXXGDWKXXFT near the C-terminal end (Figure 1) [4,5]. Since all STs use the sulphuryl donor PAPS, it is thought that conserved amino acids are involved in PAPS binding and several studies have addressed this hypothesis. Site-directed mutagenesis within the C-terminal region GISGDWKN in guinea pig oestrogen ST markedly affected the  $K_m$  for PAPS and confirmed that this part of the amino acid sequence is critical for PAPS binding [6,7]. Marsolais and Varin [8] also showed that the arginine in the RKGXXGDWKXXFT motif at the C-terminal end of flavonol 3-ST is crucial for PAPS binding. This supports the earlier studies by Borchardt et al. [9,10], which suggested that arginine residue(s) are important in the sulphuryl-transfer reaction. Recently, deduction of the first ST crystal structure by Kakuta and co-workers [11] has implicated that KSGTT in the conserved N-terminal motif and RKG in the conserved C-terminal motif are involved in PAPS

binding in mouse oestrogen ST. Furthermore, R130 and S138 from the central region were also found to contribute to PAPS binding (Figure 1).

The distinct substrate specificities displayed within the ST family [12] suggest that the structure of the substrate-binding site has undergone divergence during evolution. Therefore, the amino acid residues that contribute to substrate binding are likely to reside in regions that display the most variability across different members of the ST family. Chimaeric-construct studies of flavonol STs [13] and rat hydroxysteroid STs [14] have suggested that the central regions spanning amino acids 92–194 and 102–164, respectively, determine the substrate specificity of these STs. Involvement of the amino acids within this region in substrate binding was confirmed by Kakuta et al. [11] in their study of the binding of oestradiol to the mouse oestrogen ST. This study also indicated the importance of amino acids at the C-terminal end (M243, M247 and M248) in oestradiol binding.

In our laboratory we have cloned five human aryl (phenol) STs: HAST (human aryl sulphotransferase) 1, HAST2, HAST3, HAST4 and HAST4v [15–17]. According to a proposed nomenclature system (Third International Sulfation Workshop, Drymen, Scotland, September 1996) these would be named SULT1A1 (HAST1 and HAST2), SULT1A2 (HAST4 and HAST4v) and SULT1A3 (HAST3). HAST1 and HAST2 encode identical proteins, but vary in their 5' non-coding sequence. The remaining HASTs share greater than 90% sequence identity at the amino acid level (Figure 1) but vary markedly in their substrate preferences. For example, HAST1 and HAST3 are

Abbreviations used: HAST, human aryl sulphotransferase; PAPS, 3'-phosphoadenosine 5'-phosphosulphate; ST, sulphotransferase.

<sup>1</sup> To whom correspondence should be addressed (e-mail mcmanus@plpk.uq.edu.au).



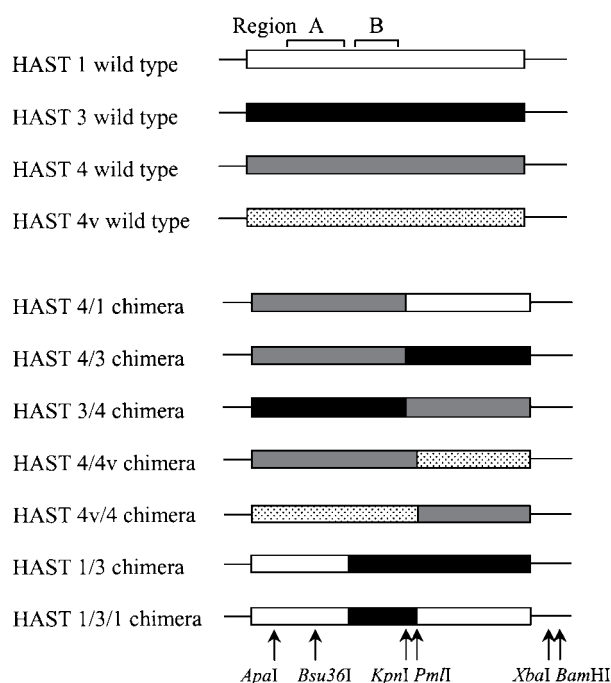


**Figure 2** HASTs and their chimaeric constructs

Regions A and B are as shown in Figure 1.

### Site-directed mutagenesis

Site-directed mutagenesis was performed by PCR using *Pfu* DNA polymerase and the QuikChange<sup>®</sup> site-directed mutagenesis method (Stratagene, La Jolla, CA, U.S.A.). HAST1 cDNA inserted into the pBluescript vector was used as the original DNA template. Oligonucleotides used for mutagenesis are shown below. (Mutated codons are underlined and lower case letters indicate a base change from wild type. In some cases silent mutations were introduced to create or delete an endonuclease recognition site, which was used to identify mutant clones): S44N, 5'-GATGACCTGCTCATCAACACCTACCC-AAGTCC-3'; H71N, 5'-GACCTGGAGAAGTGTaACCGgG-CTCCCATC-3'; F76Y, 5'-GAGCTCCCATCTaCATGCGG-GTGCCCTTC-3'; M77V, 5'-CCGAGCTCCCATCTTCgTaC-GGGTGCCCTTCCTTG-3'; F84V, 5'-GCCCTTCCTTGA-GgTCAAAGCCCCAGG-3'; K85N, 5'-GTGCCCTTCCTT-GAaTTCAAcGCCCCAGGGATTCCC-3'; A86D, 5'-GGT-GCCCTTCCTTGAaTTCAAAGaCCCAGGGATTCCC-3'; I89E, 5'-CCTTGAGTTCAAAGCCCCAGGGgagCCgTCAG-GGATGGAGACTCTG-3'; M93L, 5'-CCCAGGGATTCCC-TCAGGGgCgGAGACTCTGAAAGAC-3'; A101P, 5'-CTGA-AAGACACACCGcCCCCACGACTCCTG-3'; L105I, 5'-CC-GGCCCCACGACTCaTcAAGACACACCTGCC-3'; T107S, 5'-CACGACTCCTGAAGtCACACCTGCCCTG-3'; and A146E, 5'-CCAATTCTACCACATGGgagAAGGTGCACCC-TGAGCC-3'.

*Escherichia coli* cells (HB101 strain) were transformed with the resultant PCR products (i.e. amplified plasmids with mutated cDNAs). Single colonies were isolated and screened for the presence of the desired mutated sequence. In order to limit the size of the PCR fragment in which additional and unwanted mutations could have occurred, unique restriction-enzyme recognition sites (*Apa*I and *Pml*I or *Bsu*36I, Figure 2) were used to

excise a 450-bp or 180-bp fragment that was subcloned into wild-type HAST1 in the pCMV5 vector.

### Restriction-digestion analysis and DNA sequencing

The cDNA sequences of chimaeric constructs were confirmed by restriction-digestion analysis. All nucleotide bases of the subcloned 450-bp or 180-bp fragments of mutated HAST1 cDNA were confirmed using the T7 Sequenase Version 2.0 DNA Sequencing Kit (Amersham Life Sciences, Cleveland, OH, U.S.A.) or the automated ABI PRISM<sup>™</sup> Dye Terminator Cycle Sequencing Ready Reaction sequencing protocol (Perkin-Elmer, Foster City, CA, U.S.A.).

### Expression of recombinant ST chimaeras and mutants

Large-scale plasmid DNA preparations of wild-type, chimaeric and mutant HASTs were obtained from *E. coli* HB101 cells. The DNA was purified by CsCl-gradient centrifugation or Wizard JETstar purification columns (Promega). COS-7 cells were transfected with the purified DNA using the DEAE dextran method as described previously [18].

### Protein detection by immunoblotting

Total protein concentration of the harvested COS-7 cells containing expressed ST protein was determined by the method of Lowry et al. [20] with BSA as the standard. Proteins were separated by SDS/PAGE and transferred to nitrocellulose membrane using a Bio-Rad Trans-Blot<sup>®</sup> Cell (Bio-Rad, Regents Park, NSW, Australia) [21]. Immunodetection of expressed protein was performed using an anti-HAST1 antibody which has been shown to recognize all the expressed HASTs in our laboratory.

### ST assays

Substrate specificities of the wild-type, chimaeric and mutant proteins towards *p*-nitrophenol, dopamine and PAPS were measured as described by Foldes and Meek [22]. The incubation mixtures contained 10 mM phosphate buffer (pH 7.0), either *p*-nitrophenol (0.03  $\mu$ M–8 mM) or dopamine (0.4  $\mu$ M–1.6 mM) as substrate, 20–100  $\mu$ g of total COS-cell protein and 20 nM–20  $\mu$ M PAPS, of which 0.6 nM–0.6  $\mu$ M was [<sup>35</sup>S]PAPS. Reactions were initiated by the addition of enzyme and incubated for 30 min at 37 °C. The monoamine oxidase inhibitor pargyline (1 mM) was included when dopamine was used as the substrate. Assays were performed in duplicate and corrected for background activity using controls which contained no substrate. Linearity of product formation with respect to time and protein concentration was determined for both *p*-nitrophenol and dopamine.

### Analysis of kinetic data

The apparent kinetic constants for PAPS, dopamine and *p*-nitrophenol were determined by fitting the Michaelis–Menten equation to the data. In experiments where the concentration of both PAPS and the acceptor substrate (A) were varied, eqn. (1) was fitted to the data. Fitting of equations was achieved via non-linear regression using the program GraphPad Prism (AMPL

software, San Diego, CA, U.S.A.) or an adaptation of DNRP53 [23]:

$v =$

$$v = \frac{V_{\max}}{1 + K_m(A)/[A] + K_m(PAPS)/[PAPS] + K_m(A)K_i(PAPS)/[A][PAPS]} \quad (1)$$

## RESULTS AND DISCUSSION

The human aryl STs HAST1, HAST3, HAST4 and HAST4v share more than 90% sequence identity at the amino acid level (Figure 1) but vary markedly in substrate specificities towards *p*-nitrophenol and dopamine. Amino acid alignments of HASTs show at least two regions of high sequence variation, Regions A (amino acids 44–107) and B (amino acids 132–164) (Figure 1). The involvement of amino acids in these regions in the substrate preferences of HAST enzymes was investigated by kinetic analysis of HAST chimaeras and specific mutants of HAST1.

### Construction and expression of chimaeric HAST proteins

A range of different HAST chimaeras were constructed: HAST4/1, HAST4/3, HAST3/4, HAST4/4v, HAST 4v/4, HAST1/3 and HAST1/3/1 (Figure 2). Following their expression in COS cells, the chimaeric proteins were subjected to SDS/PAGE and immunoblotting. Successful expression was observed for all seven chimaeric proteins, as seen in Figure 3. Some differences in the mobility of wild-type and chimaeric proteins were detected, despite the prediction of identical molecular masses for these proteins. For example, the band corresponding to the HAST3/4 chimaeric protein ran more slowly on SDS/PAGE than either of the component wild-type proteins. Similar differences in mobility of chimaeric HASTs on SDS/PAGE have been described previously [24].

### ST activities of chimaeric HAST proteins towards the substrates dopamine and *p*-nitrophenol

Specificities of COS-cell expressed chimaeric proteins towards the model substrates dopamine and *p*-nitrophenol were de-

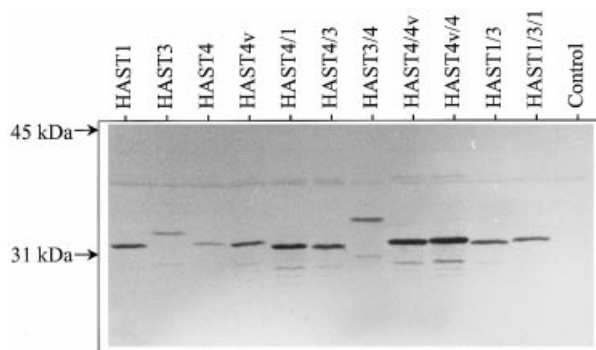


**Figure 3** Immunoblot of COS-cell expressed wild-type and chimaeric HASTs

COS-cell homogenates (50  $\mu$ g) expressing the respective constructs were loaded in each lane. The control contained COS cells transfected with the COS expression vector pCMV5 without a HAST cDNA insert. The migration of molecular-mass markers is indicated by arrows.

**Table 1** Kinetic analysis of wild-type HASTs and chimaeric constructs

Values represent best-fit values and associated standard errors obtained by fitting the Michaelis–Menten equation to rate measurements at various substrate concentrations. Calculated dopamine/*p*-nitrophenol specificity ratio, ( $V_{\max}/K_m$ ) of dopamine/( $V_{\max}/K_m$ ) of *p*-nitrophenol. No activity indicates that a  $K_m$  value could not be defined for these enzymes due to their very low specific activity towards dopamine.

Enzyme	Dopamine, $K_m$ (M)	<i>p</i> -Nitrophenol, $K_m$ (M)	Specificity ratio	PAPS, $K_m$ (M)
HAST 1	$(3.5 \pm 0.2) \times 10^{-4}$	$(4.0 \pm 1.3) \times 10^{-7}$	$3.5 \times 10^{-5}$	$(1.9 \pm 0.5) \times 10^{-6}$
HAST 3	$(1.7 \pm 0.2) \times 10^{-5}$	$(7.7 \pm 0.4) \times 10^{-3}$	$9.5 \times 10^2$	$(1.8 \pm 1.4) \times 10^{-6}$
HAST 4	No activity	$(6.9 \pm 0.6) \times 10^{-5}$	–	$(6.3 \pm 0.8) \times 10^{-6}$
HAST 4v	No activity	$(4.1 \pm 0.5) \times 10^{-6}$	–	$(2.5 \pm 0.3) \times 10^{-7}$
HAST 4/1	No activity	$(3.4 \pm 0.2) \times 10^{-6}$	–	$(4.8 \pm 0.4) \times 10^{-8}$
HAST 4/3	No activity	$(1.3 \pm 0.1) \times 10^{-6}$	–	$(4.2 \pm 0.3) \times 10^{-7}$
HAST 3/4	$(1.7 \pm 0.1) \times 10^{-5}$	$(5.1 \pm 0.8) \times 10^{-3}$	$2.3 \times 10^3$	$(3.2 \pm 0.1) \times 10^{-6}$
HAST 4/4v	No activity	$(7.2 \pm 0.6) \times 10^{-6}$	–	$(5.5 \pm 0.4) \times 10^{-7}$
HAST 4v/4	No activity	$(3.0 \pm 0.3) \times 10^{-5}$	–	$(4.1 \pm 0.9) \times 10^{-6}$
HAST 1/3	$(2.4 \pm 0.3) \times 10^{-4}$	$(5.2 \pm 0.6) \times 10^{-5}$	$5.6 \times 10^{-2}$	$(1.1 \pm 0.1) \times 10^{-6}$
HAST 1/3/1	$(4.8 \pm 0.4) \times 10^{-4}$	$(5.0 \pm 0.6) \times 10^{-5}$	$1.0 \times 10^{-1}$	$(2.2 \pm 0.2) \times 10^{-7}$

termined (Table 1). The  $K_m$  values obtained are useful for comparison of the substrate preferences of different enzymes. However, they do not represent a direct measure of substrate affinity because  $K_m$  depends on rate constants throughout the catalytic pathway, including catalysis itself and product release. A better indicator of specificity is the ratio  $V_{\max}/K_m$ , known as the specificity constant [25]. Values of this constant were calculated for HAST1, HAST3 and each of the chimaeras for their catalysis of dopamine and *p*-nitrophenol. Valid comparisons cannot be made between the various enzymes because  $V_{\max}$  depends on the amount of enzyme, which may differ between preparations. However, for any given enzyme, the ratio of these specificity constants (dopamine/*p*-nitrophenol) can be compared and these values clearly illustrate the substrate preferences of HAST1 and HAST3 (Table 1). By this measure HAST3 shows a preference for dopamine by a factor of 950, whereas HAST1 has a very large preference for *p*-nitrophenol. The HAST3/4 chimaera has a specificity ratio that is similar to that of HAST3. No enzyme activity towards dopamine was detectable for either HAST4/1 or HAST4/3, as is the case for wild-type HAST4. These results indicate that the substrate specificity is determined within the N-terminal portion of HAST proteins, which contains the two regions of high sequence variation, Regions A and B (Figure 1). This suggests that non-conserved amino acid(s) within these two regions are responsible for the distinct substrate preferences of HASTs.

The HAST1/3 and HAST1/3/1 chimaeras both exhibited  $K_m$  values comparable with wild-type HAST1 with dopamine as the substrate. The  $K_m$  values obtained with *p*-nitrophenol were intermediate between wild-type HAST1 and HAST3. In relation to their ability to utilize *p*-nitrophenol, HAST1/3 and HAST1/3/1 resemble HAST4, but unlike HAST4 they retain their capacity to sulphonate dopamine. The data from these two chimaeras suggest that the amino acids that determine enzyme affinity towards dopamine reside within Region A and those that determine the affinity for *p*-nitrophenol reside within Regions A and B (Figure 1). Our findings therefore suggest that *p*-nitrophenol and dopamine binding is dependent on amino acid residues contributed by different regions in the HASTs. This phenomenon has been described previously by Homma et al. [26] for rat hydroxysteroid ST binding of dehydroepiandrosterone and cortisol. Further, our findings confirm those of a recent

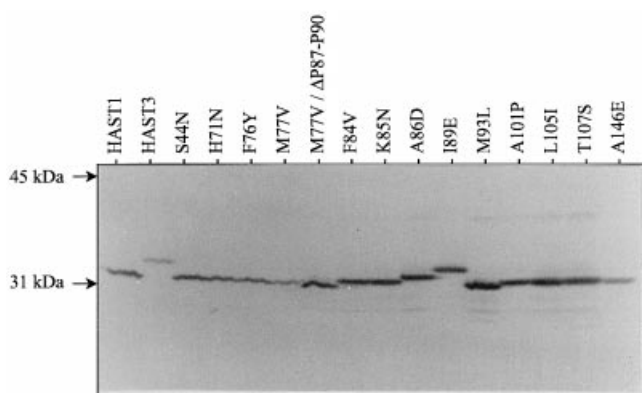


**Figure 4** Immunoblot of COS-cell expressed wild-type HAST1 and HAST3, and mutant HAST1 constructs

COS-cell homogenates (50  $\mu$ g) expressing the respective proteins were loaded in each lane. The migration of molecular-mass markers is indicated by arrows.

study by Sakakibara et al. [24], which indicated that amino acids within Regions A and B determine the substrate preferences of HAST1 and HAST3. The wild-type HAST4 and HAST4v vary by only two amino acids (T7/I and T235/N) but differ markedly in their affinity towards *p*-nitrophenol and PAPS [17]. The chimaeric constructs of these proteins contain a single amino acid change compared with their wild types (e.g. HAST4/4v is HAST4 with T235  $\rightarrow$  N), as described previously [27]. This single amino acid change led to reversal of  $K_m$  values for *p*-nitrophenol when compared with their wild-types (Table 1). This shows that the amino acid at position 235 in the C-terminal region of HAST4 and HAST4v is involved in the affinity for *p*-nitrophenol. If we assume that the crystal structure of the mouse oestrogen ST corresponds closely to those of the HASTs, this amino acid seems likely to be able to affect substrate binding as it is in close proximity to the proposed substrate-binding pocket [11]. Neither wild-type HAST4 nor HAST4v, or the chimaeras of these two showed any detectable activity towards dopamine as a substrate.

#### ST activities of chimaeric HAST proteins towards PAPS

The wild-type HASTs and the HAST chimaera activities towards the sulphuryl donor PAPS were determined. The  $K_m$  values of the wild-type HASTs varied from 0.25 to 6.3  $\mu$ M PAPS (Table 1). Of the chimaeric constructs, only the HAST4/4v and HAST4v/4 proteins showed a substantial change in affinity towards PAPS (35 fold). As described above, these proteins differ by only one amino acid (T235/N) compared with the wild type. The findings therefore suggest that residue 235 is involved in determining the affinity of HAST4 and HAST4v towards PAPS. The affinity of HAST4/1, HAST4/3 and HAST3/4 towards PAPS revealed  $K_m$  values comparable with their C-terminal wild types; HAST1, HAST3 and HAST4, respectively. This may result from the influence of amino acid (N235T) as described above, as all the proteins with a Thr at this position have high  $K_m$  values (like HAST4), and all with an Asn at this position have low  $K_m$  values, towards PAPS (like HAST1, HAST3 and HAST4v). As mentioned above, the residue at position 235 in the mouse oestrogen ST crystal structure [11] is in close proximity to the proposed binding sites of both the acceptor substrate and PAPS. Our findings therefore support the importance of this residue in the binding pocket(s), as its alteration significantly

affects affinity of the HAST enzymes for both PAPS and acceptor substrates.

#### Construction and expression of mutant HAST proteins

The wild-type HAST1 and HAST3 enzymes have very distinct substrate specificities towards dopamine and *p*-nitrophenol, although they share 93% identity at the amino acid level. This corresponds to only 21 differences of a total of 295 amino acids in HAST1 and HAST3 (Figure 1). Analysis of the HAST chimaeras described in the previous sections revealed that the amino acid(s) responsible for determining the affinity of HAST proteins for dopamine and *p*-nitrophenol are located within Regions A and B. We therefore constructed 13 mutant HAST1 proteins within these regions. Each of the 13 amino acids in HAST1 were exchanged for the amino acid at the corresponding location in HAST3 (Figure 1). Mutant proteins were expressed in COS cells and subjected to SDS/PAGE and immunoblotting. Successful expression was observed for all mutant proteins (Figure 4). The mobilities of each of the 13 expressed mutant proteins are equivalent to that of wild-type HAST1 except for I89E, which runs similarly to wild-type HAST3. This is consistent with Sakakibara and co-workers' [24] observation that the amino acid(s) responsible for the slow mobility of HAST3 reside within their Region I, which is incorporated in our Region A (Figure 1) and includes the amino acid at position 89.

#### ST activities of mutant HAST proteins towards the substrates dopamine and *p*-nitrophenol

Single amino acids were exchanged in wild-type HAST1 to the corresponding amino acid in wild-type HAST3 to enable investigation of the influence of these amino acids in determining affinity towards the model substrates dopamine and *p*-nitrophenol. One single amino acid change in HAST1 (A146E) was able to alter the  $K_m$  value for *p*-nitrophenol from 0.4  $\mu$ M to 1.7 mM. In comparison, HAST3 has a  $K_m$  value for *p*-nitrophenol of 7.7 mM. Therefore we are able to suggest that this single amino acid change (A146E) in HAST1 gives the expressed mutant protein HAST3-like characteristics with respect to *p*-nitrophenol sulphonation. The mutant A86D shows a small decrease in affinity towards *p*-nitrophenol compared with HAST1 ( $K_m = 3.1 \mu$ M versus 0.4  $\mu$ M) and may therefore also affect *p*-nitrophenol binding. Interestingly, this mutant, along with mutants S44N, F84V and A146E, shows undetectable activity towards dopamine as a substrate. These findings indicate that the amino acids at positions 44, 84, 86 and 146 influence the binding of dopamine by HAST1. Although none of the single amino acid changes were able to convert the HAST1 substrate specificities to resemble those of HAST3 with respect to dopamine, these amino acids may still be involved in determining the affinity for this substrate. It may be necessary to change more than one of these amino acids in combination to alter the substrate specificities for HASTs with regard to dopamine. This is consistent with the findings of Marsolais and Varin [28], where single amino acid changes were not sufficient for reversal of the substrate specificities of flavonol STs.

The recently published crystal structure of a mouse oestrogen ST [11] reports a loop region between  $\beta$ -sheets 5 and 6 corresponding to four amino acids, P87–P90, within Region A of HASTs (Figure 1). This loop region may participate in the substrate binding of STs since it resides in close proximity to the substrate-binding pocket [11]. We therefore constructed a

**Table 2 Kinetic analysis of wild-type HAST 1 and HAST 3 and single amino acid HAST1 mutants**

For dopamine, values represent best-fit values and associated standard errors obtained by fitting the Michaelis–Menten equation to rate measurements at various substrate concentrations. For *p*-nitrophenol  $K_m$ , PAPS  $K_m$  and PAPS  $K_i$  values represent best-fit values and associated standard errors obtained by fitting eqn. (1) to rate measurements at various substrate concentrations (shown in Figure 5). Calculated dopamine/*p*-nitrophenol specificity ratio, ( $V_{max}/K_m$ ) of dopamine/( $V_{max}/K_m$ ) of *p*-nitrophenol. No activity, indicates that a  $K_m$  value could not be defined for these enzymes due to their very low specific activity towards dopamine. n.d., not determined.

Enzyme	Dopamine, $K_m$ (M)	<i>p</i> -Nitrophenol, $K_m$ (M)	Specificity ratio	PAPS, $K_m$ (M)	PAPS, $K_i$ (M)
HAST 1	$(3.5 \pm 0.2) \times 10^{-4}$	$(4.0 \pm 1.3) \times 10^{-7}$	$3.5 \times 10^{-5}$	$(1.9 \pm 0.5) \times 10^{-6}$	$(1.0 \pm 0.4) \times 10^{-6}$
HAST 3	$(1.7 \pm 0.2) \times 10^{-5}$	$(7.7 \pm 0.4) \times 10^{-3}$	$9.5 \times 10^2$	$(1.8 \pm 1.4) \times 10^{-6}$	$(2.0 \pm 0.7) \times 10^{-6}$
S44N	No activity	$(5.1 \pm 0.7) \times 10^{-7}$	–	$(1.3 \pm 0.2) \times 10^{-6}$	$(3.3 \pm 0.7) \times 10^{-6}$
H71N	$(3.2 \pm 1.2) \times 10^{-4}$	$(6.2 \pm 1.5) \times 10^{-8}$	$1.9 \times 10^{-4}$	$(2.7 \pm 0.7) \times 10^{-8}$	$(4.0 \pm 1.7) \times 10^{-8}$
F76Y	$(7.3 \pm 3.0) \times 10^{-4}$	$(1.6 \pm 0.2) \times 10^{-7}$	$2.8 \times 10^{-5}$	$(1.6 \pm 1.1) \times 10^{-7}$	$(5.2 \pm 3.0) \times 10^{-7}$
M77V	$(1.3 \pm 0.1) \times 10^{-3}$	$(1.2 \pm 0.6) \times 10^{-7}$	$1.4 \times 10^{-4}$	$(1.9 \pm 0.8) \times 10^{-7}$	$(1.3 \pm 0.8) \times 10^{-6}$
M77V/ $\Delta$ P87-P90	$(9.0 \pm 1.7) \times 10^{-7}$	$(2.1 \pm 0.3) \times 10^{-3}$	$2.3 \times 10^3$	n.d.	n.d.
F84V	No activity	$(6.6 \pm 1.2) \times 10^{-7}$	–	$(1.1 \pm 0.2) \times 10^{-6}$	$(1.0 \pm 0.3) \times 10^{-5}$
K85N	$(2.4 \pm 0.3) \times 10^{-4}$	$(6.1 \pm 1.6) \times 10^{-7}$	$3.6 \times 10^{-5}$	$(5.6 \pm 1.2) \times 10^{-6}$	$(5.1 \pm 1.9) \times 10^{-6}$
A86D	No activity	$(3.1 \pm 1.0) \times 10^{-6}$	–	$(3.0 \pm 0.8) \times 10^{-6}$	$(2.1 \pm 0.7) \times 10^{-5}$
I89E	$(1.5 \pm 0.3) \times 10^{-4}$	$(1.5 \pm 0.1) \times 10^{-6}$	$2.3 \times 10^{-4}$	$(2.4 \pm 0.3) \times 10^{-6}$	$(5.0 \pm 0.6) \times 10^{-6}$
M93L	$(1.0 \pm 0.3) \times 10^{-4}$	$(4.3 \pm 0.6) \times 10^{-7}$	$4.2 \times 10^{-5}$	$(2.3 \pm 0.2) \times 10^{-6}$	$(1.9 \pm 0.5) \times 10^{-6}$
A101P	$(6.0 \pm 0.4) \times 10^{-4}$	$(2.5 \pm 0.2) \times 10^{-7}$	$5.2 \times 10^{-5}$	$(8.9 \pm 0.8) \times 10^{-7}$	$(1.0 \pm 0.2) \times 10^{-6}$
L105I	$(3.2 \pm 0.7) \times 10^{-4}$	$(1.0 \pm 0.1) \times 10^{-6}$	$7.6 \times 10^{-5}$	$(2.2 \pm 0.2) \times 10^{-6}$	$(3.0 \pm 0.7) \times 10^{-6}$
T107S	$(1.1 \pm 0.4) \times 10^{-4}$	$(6.0 \pm 0.4) \times 10^{-7}$	$1.6 \times 10^{-4}$	$(1.1 \pm 0.1) \times 10^{-6}$	$(1.5 \pm 0.2) \times 10^{-6}$
A146E	No activity	$(1.1 \pm 0.2) \times 10^{-3}$	–	$(3.8 \pm 2.4) \times 10^{-7}$	$(6.4 \pm 1.6) \times 10^{-6}$

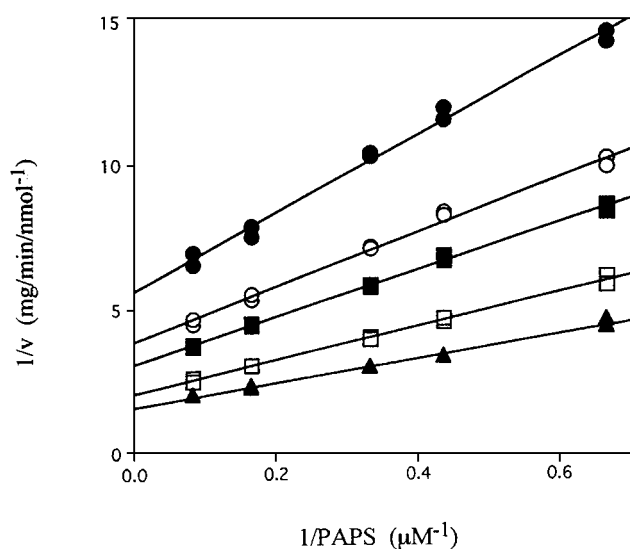


**Figure 5** A representative double-reciprocal plot of the sulphonation of *p*-nitrophenol by mutant HAST1 protein (L105I)

The different symbols represent fixed concentrations of *p*-nitrophenol of 0.3 (●), 0.45 (○), 0.6 (■), 1.2 (□) and 2.4  $\mu$ M (▲). The intersecting lines represent the best fit of eqn. (1) to the data and indicate that the sulphonation reaction occurs according to a sequential Bi-Bi mechanism.

mutant (M77V) with these four amino acids deleted (M77V/ $\Delta$ P87-P90). The protein encoded by this construct was successfully expressed in COS cells (Figure 4) and the substrate specificities towards dopamine and *p*-nitrophenol were determined. The M77V/ $\Delta$ P87-P90 protein shows substrate specificities more similar to wild-type HAST3 than to HAST1, whereas the M77V mutant alone showed substrate specificities corresponding to wild-type HAST1 (Table 2). These results support our hypothesis that these four amino acids (P87–P90)

play an important role in the substrate binding of HAST1. Interestingly, alignment of HASTs with hydroxysteroid STs show that this latter subfamily lacks the amino acids in the corresponding positions (P87–S91) [2]. These amino acids may therefore play a role in determining the substrate specificities of these two enzyme families.

#### ST activities of mutant HAST proteins towards PAPS

The sulphonation reaction is generally thought to occur according to an ordered sequential Bi-Bi mechanism, with the sulphuryl donor (PAPS) being the first substrate to bind to the ST enzyme followed by the sulphuryl-acceptor substrate [29]. However, it should be noted that there is still some debate as to whether the binding of PAPS and the acceptor substrate is ordered or random [29–32]. In either case, the true dissociation constant ( $K_i$ ) for PAPS can be determined by experiments in which the concentration of both substrates is varied and the results analysed by eqn. (1). Such experiments were performed for wild-type HAST1 and HAST3, and the HAST1 mutants. The double-reciprocal plots of wild-type and mutant proteins all show intersecting lines with varying concentrations of *p*-nitrophenol, confirming that the sulphonation by HASTs occurs according to a sequential mechanism (Figure 5). Wild-type HAST1 and HAST3 have comparable  $K_i$  values for PAPS (1.0 and 2.0  $\mu$ M, respectively). Similar  $K_i$  values were observed for mutants F76Y, M77V, M93L, A101P and T107S. The mutants S44N, K85N, I89E, L105I and A146E all had slightly elevated  $K_i$  values compared with the wild types. Mutants F84V and A86D showed significantly increased  $K_i$  values for PAPS (10- and 20-fold, respectively), whereas mutant H71N showed a 25-fold decrease. These results suggest that these single amino acid changes affect PAPS binding by HASTs and that co-ordinated amino acid interactions are responsible for the overall similarity between HAST1 and HAST3 with respect to PAPS binding.

In conclusion, we have shown with chimaeric constructs that the amino acid residues which are influential in determining the substrate specificities of HASTs reside within the N-terminal region of these enzymes. In HAST1 a single amino acid change

(A146E) was able to change the affinity for *p*-nitrophenol to that of HAST3. With respect to dopamine, the substrate specificity of HAST1 could not be converted into that of HAST3 with single amino acid changes. However, a number of the mutants interfered with the substrate binding of wild-type HAST1, as shown by elevated  $K_i$  values towards PAPS and, in some cases, loss of activity towards dopamine. We suggest that a number of amino acids interact to determine the affinity of HASTs towards dopamine. Furthermore, we were able to reverse the substrate specificity of a HAST protein by introducing a four-amino acid deletion, at a position thought to be in close proximity to the substrate-binding pocket. Investigations of the HAST substrate-binding pocket are currently in progress in our laboratory.

This research was supported by the National Health and Medical Research Council of Australia (grant no. 951291). We thank Dr. M. E. Veronese for constructing three of the chimaeric plasmids and Dr. R. Bolton and L. Bidwell for critical reading of the manuscript.

## REFERENCES

- Falany, C. N. (1997) *FASEB J.* **11**, 206–216
- Rikke, B. A. and Roy, A. K. (1996) *Biochim. Biophys. Acta* **1307**, 331–338
- Weinshilboum, R. M. and Otterness, D. (1994) in *Handbook of Experimental Pharmacology* (Kauffman, F. C., ed.), pp. 45–78, Springer-Verlag, Berlin
- Weinshilboum, R. M., Otterness, D. M., Aksoy, I. A., Wood, T. C., Her, C. and Raftogianis, R. B. (1997) *FASEB J.* **11**, 3–14
- Varin, L., Marsolais, F., Richard, M. and Rouleau, M. (1997) *FASEB J.* **11**, 517–525
- Komatsu, K., Driscoll, W. J., Koh, Y. C. and Strott, C. A. (1994) *Biochem. Biophys. Res. Commun.* **204**, 1178–1185
- Driscoll, W. J., Komatsu, K. and Strott, C. A. (1995) *Proc. Natl. Acad. Sci. U.S.A.* **92**, 12328–12332
- Marsolais, F. and Varin, L. (1995) *J. Biol. Chem.* **270**, 30458–30463
- Borchardt, R. T. and Schasteen, C. S. (1977) *Biochem. Biophys. Res. Commun.* **78**, 1067–1073
- Borchardt, R. T., Schasteen, C. S. and Wu, S.E. (1982) *Biochim. Biophys. Acta* **708**, 280–293
- Kakuta, Y., Pedersen, L. G., Carter, C. W., Negishi, M. and Pedersen, L. C. (1997) *Nat. Struct. Biol.* **4**, 904–908
- Coughtrie, M. (1996) *Hum. Exp. Toxicol.* **15**, 547–555
- Varin, L., Marsolais, F. and Brisson, N. (1995) *J. Biol. Chem.* **270**, 12498–12502
- Tamura, M., Morioka, Y., Homma, H. and Matsui, M. (1997) *Arch. Biochem. Biophys.* **341**, 309–314
- Zhu, X., Veronese, M. E., Sansom, L. N. and McManus, M. E. (1993) *Biochem. Biophys. Res. Commun.* **192**, 671–676
- Zhu, X., Veronese, M. E., Bernard, C. C. A., Sansom, L. N. and McManus, M. E. (1993) *Biochem. Biophys. Res. Commun.* **195**, 120–127
- Zhu, X., Veronese, M. E., Iocco, P. and McManus, M. E. (1996) *Int. J. Biochem. Cell Biol.* **28**, 565–571
- Veronese, M. E., Burgess, W., Zhu, X. and McManus, M. E. (1994) *Biochem. J.* **302**, 497–502
- Gaedigk, A., Lekas, P., Berchuk, M. and Grant, D. (1998) *Chem. Biol. Int.* **109**, 43–52
- Lowry, O. H., Rosebrough, N. J., Farr, A. L. and Randall, R. J. (1951) *J. Biol. Chem.* **193**, 265–275
- Towbin, H., Staehelin, T. and Gordon, J. (1979) *Proc. Natl. Acad. Sci. U.S.A.* **76**, 4350–4354
- Foldes, A. and Meek, J. L. (1973) *Biochim. Biophys. Acta* **327**, 365–374
- Duggleby, R. G. (1984) *Comput. Biol. Med.* **14**, 447–455
- Sakakibara, Y., Takami, Y., Nakayama, T., Suiko, M. and Liu, M.-C. (1998) *J. Biol. Chem.* **273**, 6242–6247
- Cornish-Bowden, A. (1995) *Fundamentals of Enzyme Kinetics*, Portland Press Ltd., London
- Homma, H., Ogawa, K., Hirono, K., Morioka, Y., Hirota, M., Tanahashi, I. and Matsui, M. (1996) *Biochim. Biophys. Acta* **1296**, 159–166
- Brix, L. A., Nicoll, R., Zhu, X. and McManus, M. E. (1998) *Chem. Biol. Interact.* **109**, 123–127
- Marsolais, F. and Varin, L. (1997) *Eur. J. Biochem.* **247**, 1056–1062
- Pennings, E. J., Vrieling, R. and van Kempen, G. M. (1978) *Biochem. J.* **173**, 299–307
- Varin, L. and Ibrahim, R. K. (1992) *J. Biol. Chem.* **267**, 1858–1863
- Duffel, M. W. and Jakoby, W. B. (1981) *J. Biol. Chem.* **256**, 11123–11127
- Zhang, H., Varmalova, O., Vargas, F. M., Falany, C. N. and Leyh, T. S. (1998) *J. Biol. Chem.* **273**, 10888–10892

Received 4 August 1998/8 October 1998; accepted 3 November 1998